ChemComm
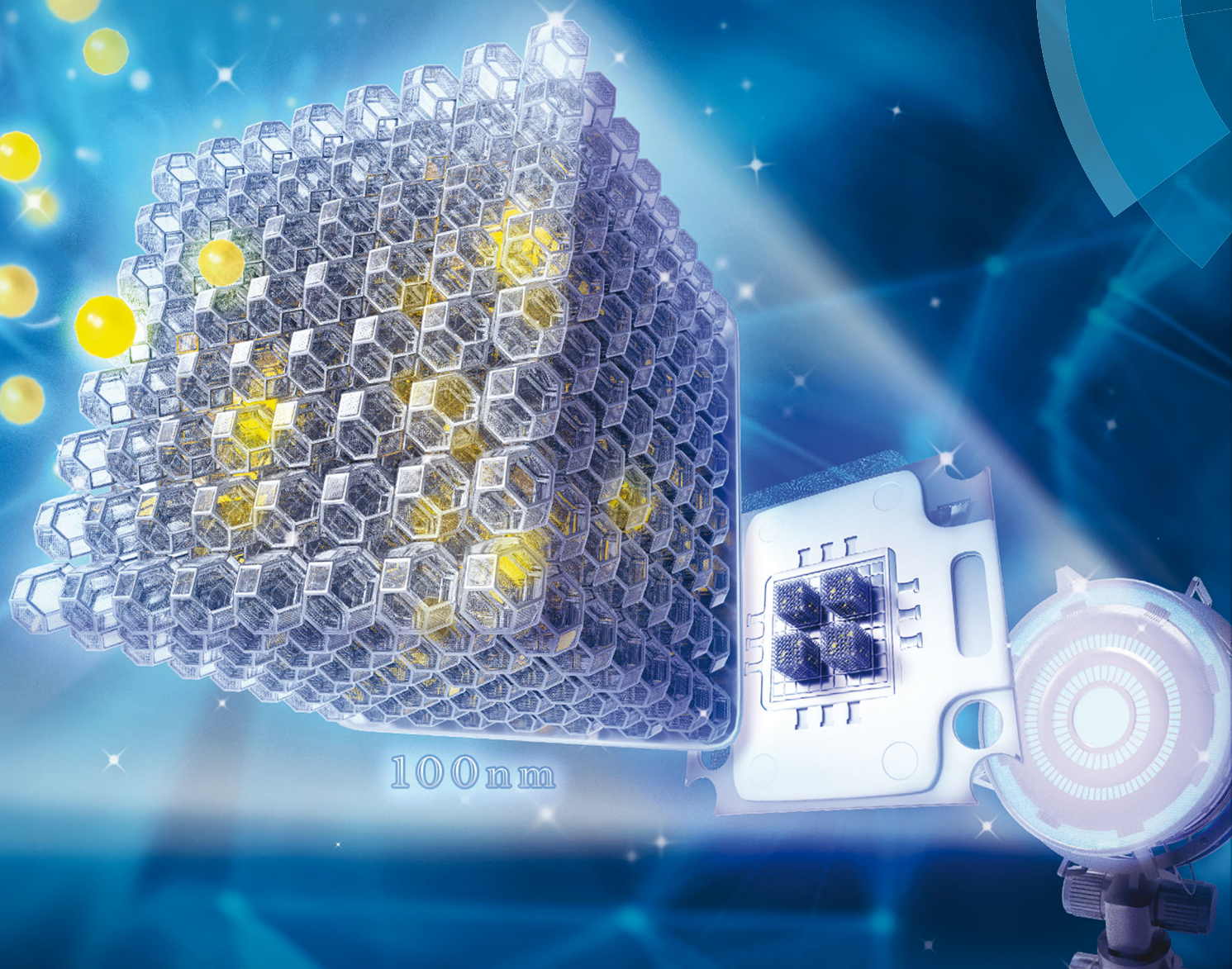
Chemical Communications

rsc.li/chemcomm

100 nm

ROYAL SOCIETY OF CHEMISTRY | Celebrating IYPT 2019

COMMUNICATION
Jing Li *et al.*
Encapsulation of yellow phosphors into nanocrystalline metal–organic frameworks for blue-excitable white light emission

COMMUNICATION

Check for updates

Encapsulation of yellow phosphors into nanocrystalline metal–organic frameworks for blue-excitable white light emission†

Xiao-Yuan Liu, [ID] [ab] Yang Li, [c] Chia-Kuang Tsung [ID] [c] and Jing Li [ID] ★[ba]
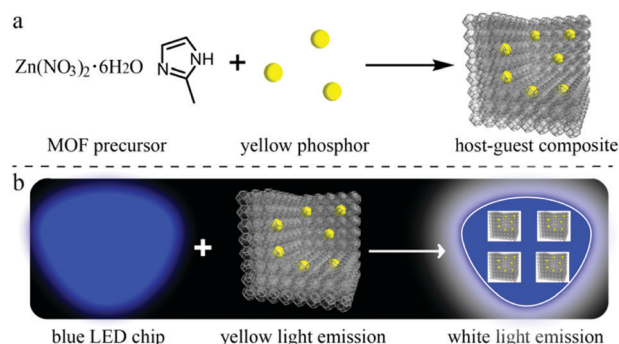
Host–guest based highly emissive and solution processable nano-composites are achieved by *in situ* encapsulation of yellow-emitting molecular dyes into ZIF-8 and UiO-66 during their nano-crystal formation, which can be effectively excited by blue light to generate white light.

In recent years, metal–organic framework (MOF) based host–guest composite materials have received tremendous attention, largely because of their multi-fold tunability. In addition to modifiable chemical composition and crystal structure as commonly observed for conventional MOFs, the composite materials have an added advantage, namely nearly unlimited choice of guest species. Studies have demonstrated their potential in various important applications, including, but not limited to catalysis,[1–5] drug delivery,[6,7] and chemical sensing.[8] Dye encapsulated MOF (dye@MOF) composites are particularly promising in producing high quality white light.[9–18] Usually, the preparation of this kind of host–guest composite starts from the synthesis of pristine MOFs, followed by ion exchange to incorporate the dye molecules into the MOF structure.[9,10,14,19,20] Unlike other MOF-based white light emitting materials,[21–24] the dye@MOF composites do not contain complex ligands and/or rare-earth elements. More importantly, the composites typically show remarkable enhancement in their solid state luminescence over pristine dye molecules, as the host–guest systems can effectively suppress the aggregation caused quenching (ACQ) by confining and isolating individual dye molecules within the MOF pores.

However, further improvement is required to overcome several shortcomings of these host–guest composites. First of all, the two-step preparation method mentioned above is time-consuming, and more problematically, the guest molecules must be smaller than the aperture size in order to enter the MOF pores, which will not only restrict the choice of guests but also cause severe guest leakage.[9,11,13] Secondly, the synthesis of strongly luminescent MOFs often requires the use of expensive reagents and in most cases, a UV light source is needed to excite them effectively. Third, most of the reported dye@MOFs are macro-sized composites, which are not suitable for device fabrication due to the lack of solution processability. These pose serious limitations for their commercial applications in the current lighting technologies. Therefore, developing alternative synthetic strategies that can address these drawbacks is very desirable.

To improve the tedious two-step synthesis and prevent the captured guest molecules from leaking out, a new and simple synthetic approach has been developed which allows trapping guest molecules *in situ* into the MOF pore space.[25] In this study, we apply this method to encapsulate two yellow-emitting dyes into the MOFs, namely zeolitic imidazolate framework 8 (ZIF-8) and UiO-66 during their crystal formation (Scheme 1, top). As the dye molecule can be effectively excited by a blue light source (450 nm), a white LED combining a blue LED chip and

[a] *Hoffmann Institute of Advanced Materials, Shenzhen Polytechnic,
7098 Liuxian Blvd, Nanshan District, Shenzhen 518055, P. R. China*

[b] *Department of Chemistry and Chemical Biology, Rutgers University,
123 Bevier Road, Piscataway, NJ 08854, USA. E-mail: jingli@rutgers.edu*

[c] *Department of Chemistry, Merkert Chemistry Center, Boston College,
2609 Beacon Street, Chestnut Hill, Massachusetts 02467, USA*

† Electronic supplementary information (ESI) available. See DOI: 10.1039/c9cc05533a

Scheme 1 A schematic diagram illustrating the synthesis of MOF and yellow phosphor based host–guest composites (top), and the generation of white light from a blue light source and a blue-excitable yellow phosphor (bottom).

the dye@MOF composite can be constructed (Scheme 1, bottom). We demonstrate that high quality nanocomposites can be formed by selecting a MOF–dye pair with comparable solubility.

Rhodamine 6G (R6G) was chosen as the yellow phosphor in this work because of its excellent yellow emission property in water solution.[26] As shown in Fig. 1c, R6G emits at 553 nm (yellow) and its fluorescence intensity first decreases slightly as the excitation wavelength increases from 365 to 420 nm. A significant and monotonic increase in the emission intensity is observed as the excitation wavelength continues to increase from 440 to 480 nm, reaching a maximum at 480 nm. This observation is consistent with its absorption spectrum (see Fig. S1, ESI†). These data confirm that R6G is an excellent yellow phosphor that can be excited most efficiently by blue light,

very similar to the commercial yellow phosphor YAG:Ce. In order to effectively trap R6G, the pore size of the MOF should be at the same length scale or larger than the molecular dimension of the dye, while its pore aperture should be significantly smaller. ZIF-8 makes a perfect candidate based on these considerations for R6G. As shown in Fig. 1a and b, the molecular size of R6G is $\sim 11 \times 16$ Å,[27] which is indeed much bigger than the aperture size of ZIF-8 (3.4 Å) and at a similar scale with the pore size of ZIF-8 (11.6 Å).[28] The R6G@ZIF-8 was then synthesized by adding R6G aqueous solution into ZIF-8 precursors to form encapsulated ZIF-8 crystals *in situ*.[25,29] The nanocrystal product was washed thoroughly using methanol. Another shell of ZIF-8 was then grown on the R6G@ZIF-8 nanocrystals to obtain R6G@ZIF-8@ZIF-8 (guest@ZIF-8[2]) to avoid any possible interference on the luminescence of the nanocrystals from the surface absorbed guests.[25,30] The solid-state fluorescence spectrum of R6G@ZIF-8[2] is similar to that of the R6G water solution, yet having a remarkable increase in the intensity under blue-light excitation (Fig. 1d). As depicted in the inset of Fig. 1d, the light-brown colored R6G@ZIF-8[2] powder sample emits bright yellow light under irradiation. The highest internal quantum yield (IQY) of 63.1% was achieved for R6G@ZIF-8[2] at a concentration of 0.0264 wt% R6G (Fig. S2–S4, ESI†) under 450 nm excitation. The formation of a high quality nanocrystal structure was confirmed by scanning electron microscopy (SEM) and powder X-ray diffraction (PXRD). Fig. 2a and b show truncated rhombic dodecahedral crystals of ZIF-8[2] and R6G@ZIF-8[2] with a uniform size distribution. The PXRD patterns of R6G@ZIF-8[2] with various amounts of R6G are nearly identical to that of simulated ZIF-8 (Fig. 2e and Fig. S5, ESI†). These results demonstrate that the *in situ* encapsulated approach has no effect on the crystal structure of ZIF-8.

It is worth noting that many of the organic phosphors with excellent light emission properties are insoluble in water and methanol, as such they cannot be encapsulated into the nano-sized ZIF-8 *in situ* using water and methanol as solvents. For example, 4,9-dibromonaphtho[2,3-*c*][1,2,5]thiadiazole (DBNT) is another yellow emitting dye (λ_{em} = 550 nm) exhibiting aggregation-induced fluorescence quenching in the solid state.[31] Unlike R6G, it is insoluble in water and only slightly soluble in methanol. However it shows good solubility in DMF. The changes in its emission intensity as a function of excitation energy follow a similar trend to R6G in water, first decreasing from 365 to 400 nm and then gradually increasing from 420 to 480 nm (Fig. 1g). The maximum fluorescence intensity achieved for blue light excitation suggests that DBNT is also a promising yellow phosphor compatible with the current WLED technology.

Due to the fact that DMF is a poor solvent for forming dye@ZIF-8 nanocrystals, UiO-66 was chosen as a MOF host for DBNT and was synthesized following a previously reported procedure.[32] As depicted in Fig. 2c and Fig. S6 (ESI†), high quality nanocrystals of UiO-66 with a uniform size distribution (~ 150–200 nm) were confirmed by SEM and transmission electron microscopy (TEM). The molecular size of DBNT is $\sim 6.3 \times 8.0$ Å, which is larger than the aperture (~ 6 Å) of UiO-66,[33] but smaller than two kinds of cages (~ 7.5 Å for the
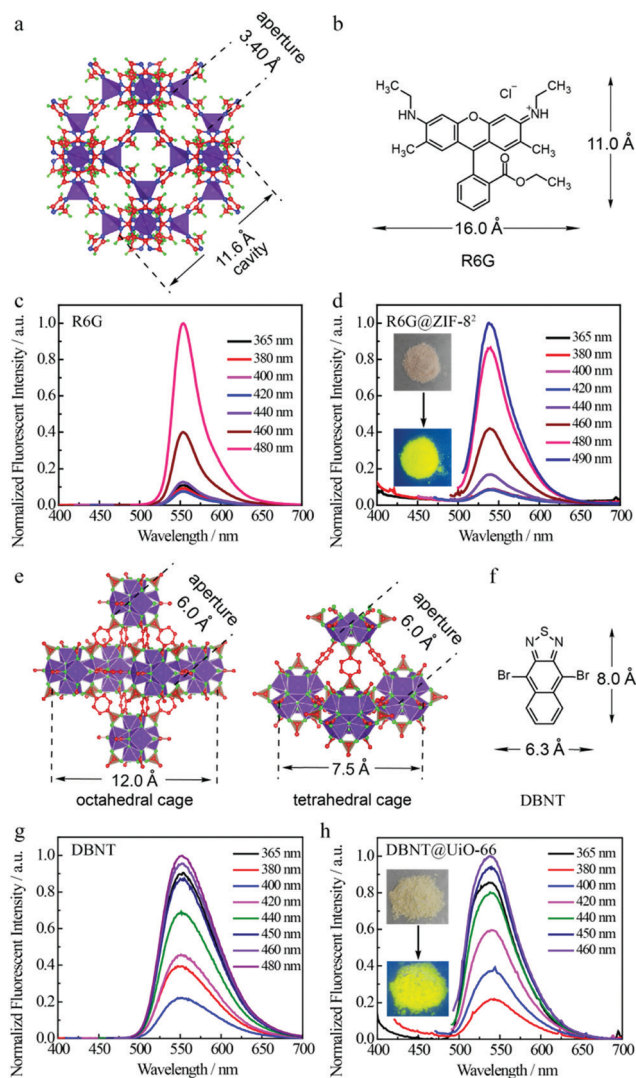

Fig. 1 The single crystal structure of (a) ZIF-8 and (e) UiO-66 with aperture and cavity sizes included; the molecular structure of (b) R6G and (f) DBNT with the dimensions; fluorescence spectra as a function of excitation energies of (c) R6G in water solution, (d) solid R6G@ZIF-8[2], (g) DBNT in DMF, and (h) solid DBNT@UiO-66; inset: (d) the photographs of R6G@ZIF-8[2] under daylight and excitation, (h) the photographs of DBNT@UiO-66 under daylight and excitation.
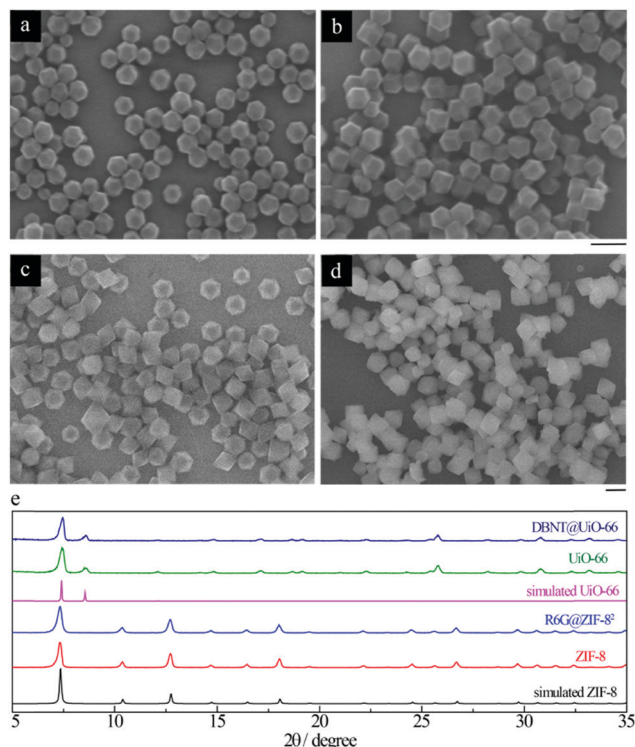
Fig. 2 The SEM images of (a) pure ZIF-8, (b) R6G@ZIF-8^2, (c) pure UiO-66 and (d) DBNT@UiO-66, scale bar: 200 nm; (e) the PXRD of simulated ZIF-8, as synthesized ZIF-8 and R6G@ZIF-8^2, simulated UiO-66, as synthesized UiO-66 and DBNT@UiO-66.
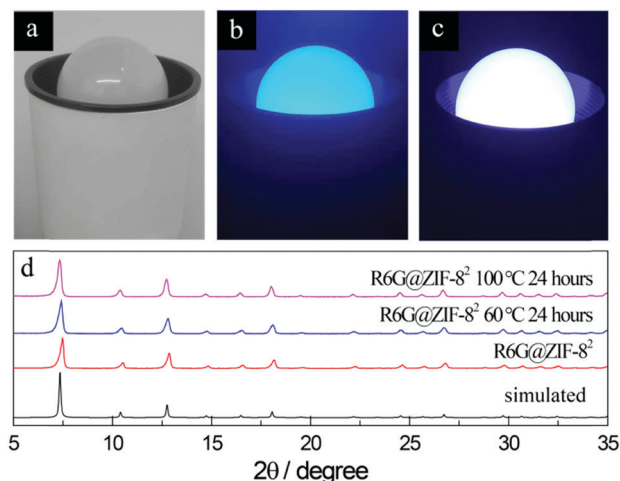

Fig. 3 Photographs of a 450 nm blue light LED lamp when the power is turned off (a) and on (b); and photograph of the LED lamp coated with R6G@ZIF-8^2 when the LED is turned on (c); (d) PXRD pattern changes before and after the treatments (heated at different temperatures for 24 hours).

tetrahedral cage, ∼12 Å for the octahedral cage) of UiO-66 (Fig. 1e and f),[34] thus, DBNT can be effectively trapped into the pores of UiO-66. The DBNT@UiO-66 nanocrystals were grown by adding DBNT/DMF into the growth solution of UiO-66. While the UiO-66 precursor solution is non-emissive and has no effect on the fluorescence of DBNT (Fig. S7, ESI†), the DBNT@UiO-66 nanocomposite sample emits yellow light (Fig. 1h, inset) with a quantum yield of 22.7% under 450 nm excitation at a DBNT concentration of 0.0105 wt%. The solid state fluorescence of DBNT@UiO-66 shows a blue-shift of ∼12 nm compared to DBNT in DMF solution and the same emission intensity dependence on the excitation wavelength (Fig. 1h). The sizes of octahedron shaped DBNT@UiO-66 nanocrystals are similar to those of pristine UiO-66 (Fig. 2c and d). The PXRD patterns of simulated, as-synthesized UiO-66, and DBNT@UiO-66 are almost identical (Fig. 2e), clearly indicating that the encapsulation process has no effect on the crystal structure of UiO-66.[35] These results demonstrate that the *in situ* encapsulation method is a general approach that is likely to be applicable to a large number of MOFs with different pore structures and dyes with various molecular sizes and solubility to prepare blue light excitable composites for the generation of white light and other colored light.

Due to the excellent emission property of R6G@ZIF-8^2, we fabricated a prototype WLED bulb by coating R6G@ZIF-8^2 onto a commercial blue light bulb (450 nm) to demonstrate the suitability of the nanocomposite dye@MOF as a yellow phosphor for a WLED device. As illustrated in Fig. 3a–c and Fig. S8 (ESI†), the R6G@ZIF-8^2 coated blue LED chip based bulb emits high quality white light. To assess its potential for commercial applications, the thermal stability of the selected dye@MOF nanocomposites was evaluated. R6G@ZIF-8^2 samples were treated under 60 and 100 °C for 24 hours. The corresponding quantum yields (QYs) decreased from 63.1% to 52.1% and 34.5%, respectively. The QY decrease is likely a result of degradation of R6G, as the PXRD patterns of the samples after stability tests remain essentially intact (Fig. 3d). Similar results were found on DBNT@UiO-66 nanocomposites.

In conclusion, we have shown in this study that different MOF hosts and a wide range of dye molecules may be selected to form dye-encapsulated nanocomposites with solubility compatibility, solution processability, and greatly enhanced solid state luminescence. We demonstrate this strategy by forming two nanocomposites using two MOFs (ZIF-8 and UiO-66) and two dyes that exhibit ACQ. Both R6G@ZIF-8^2 and DBNT@UiO-66 nanocomposites emit bright yellow light and can be effectively excited by blue-light. A high QY of 63.1% is obtained for R6G@ZIF-8^2 under 450 nm excitation, making it compatible with the current commercial WLED technology. Based on these findings, it is clear that the *in situ* encapsulation of luminescent guest molecules into MOF structures is a viable route to form solution processable nanocomposites with high solid-state luminescence efficiency. To improve the stability of these nanocomposite materials, it is important to seek high performance guest species that have strong resistance to heat and irradiation. Carbon dots (CDs) might be a promising candidate due to their cost-effective synthesis, superior optical properties, excellent biocompatibility and high stability.[36–38] Developing CDs@ZIF-8 nanocomposites as alternative phosphor materials[37,39] will be a new direction of our future research.

Conflicts of interest

There are no conflicts to declare.

Notes and references

1 M. Zhao, K. Yuan, Y. Wang, G. Li, J. Guo, L. Gu, W. Hu, H. Zhao and Z. Tang, *Nature*, 2016, **539**, 76–80.
2 C. H. Kuo, Y. Tang, L. Y. Chou, B. T. Sneed, C. N. Brodsky, Z. Zhao and C. K. Tsung, *J. Am. Chem. Soc.*, 2012, **134**, 14345–14348.
3 F. K. Shieh, S. C. Wang, C. I. Yen, C. C. Wu, S. Dutta, L. Y. Chou, J. V. Morabito, P. Hu, M. H. Hsu, K. C. Wu and C. K. Tsung, *J. Am. Chem. Soc.*, 2015, **137**, 4276–4279.
4 F. S. Liao, W. S. Lo, Y. S. Hsu, C. C. Wu, S. C. Wang, F. K. Shieh, J. V. Morabito, L. Y. Chou, K. C. Wu and C. K. Tsung, *J. Am. Chem. Soc.*, 2017, **139**, 6530–6533.
5 Z. Li, T. M. Rayder, L. Luo, J. A. Byers and C. K. Tsung, *J. Am. Chem. Soc.*, 2018, **140**, 8082–8085.
6 J. Zhuang, C.-H. Kuo, L.-Y. Chou, D.-Y. Liu, E. Weerapana and C.-K. Tsung, *ACS Nano*, 2014, **8**, 2812–2819.
7 P. Horcajada, C. Serre, M. Vallet-Regi, M. Sebban, F. Taulelle and G. Ferey, *Angew. Chem., Int. Ed.*, 2006, **45**, 5974–5978.
8 J. Deng, K. Wang, M. Wang, P. Yu and L. Mao, *J. Am. Chem. Soc.*, 2017, **139**, 5877–5882.
9 Y. Wen, T. Sheng, X. Zhu, C. Zhuo, S. Su, H. Li, S. Hu, Q. L. Zhu and X. Wu, *Adv. Mater.*, 2017, **29**, 1700778.
10 Y. Cui, T. Song, J. Yu, Y. Yang, Z. Wang and G. Qian, *Adv. Funct. Mater.*, 2015, **25**, 4796–4802.
11 C. Y. Sun, X. L. Wang, X. Zhang, C. Qin, P. Li, Z. M. Su, D. X. Zhu, G. G. Shan, K. Z. Shao, H. Wu and J. Li, *Nat. Commun.*, 2013, **4**, 2717.
12 Y. Chen, B. Yu, Y. Cui, S. Xu and J. Gong, *Chem. Mater.*, 2019, **31**, 1289–1295.
13 H. Zhao, J. Ni, J. J. Zhang, S. Q. Liu, Y. J. Sun, H. Zhou, Y. Q. Li and C. Y. Duan, *Chem. Sci.*, 2018, **9**, 2918–2926.
14 Z. Wang, C.-Y. Zhu, J.-T. Mo, P.-Y. Fu, Y.-W. Zhao, S.-Y. Yin, J.-J. Jiang, M. Pan and C.-Y. Su, *Angew. Chem., Int. Ed.*, 2019, **131**, 9854–9859.
15 W. Xie, W.-W. He, D.-Y. Du, S.-L. Li, J.-S. Qin, Z.-M. Su, C.-Y. Sun and Y.-Q. Lan, *Chem. Commun.*, 2016, **52**, 3288–3291.
16 Z. Wang, Z. Wang, B. Lin, X. Hu, Y. Wei, C. Zhang, B. An, C. Wang and W. Lin, *ACS Appl. Mater. Interfaces*, 2017, **9**, 35253–35259.
17 W. Chen, Y. Zhuang, L. Wang, Y. Lv, J. Liu, T.-L. Zhou and R.-J. Xie, *ACS Appl. Mater. Interfaces*, 2018, **10**, 18910–18917.
18 Y. Tang, T. Xia, T. Song, Y. Cui, Y. Yang and G. Qian, *Adv. Opt. Mater.*, 2018, **6**, 1800968.
19 X. Zhao, X. Bu, T. Wu, S. T. Zheng, L. Wang and P. Feng, *Nat. Commun.*, 2013, **4**, 2344.
20 X. Zhao, C. Mao, K. T. Luong, Q. Lin, Q.-G. Zhai, P. Feng and X. Bu, *Angew. Chem., Int. Ed.*, 2016, **55**, 2768–2772.
21 X. Rao, Q. Huang, X. Yang, Y. Cui, Y. Yang, C. Wu, B. Chen and G. Qian, *J. Mater. Chem.*, 2012, **22**, 3210–3214.
22 Q. Gong, Z. Hu, B. J. Deibert, T. J. Emge, S. J. Teat, D. Banerjee, B. Mussman, N. D. Rudd and J. Li, *J. Am. Chem. Soc.*, 2014, **136**, 16724–16727.
23 J. Cornelio, T. Y. Zhou, A. Alkas and S. G. Telfer, *J. Am. Chem. Soc.*, 2018, **140**, 15470–15476.
24 W. J. Newsome, S. Ayad, J. Cordova, E. W. Reinheimer, A. D. Campiglia, J. K. Harper, K. Hanson and F. J. Uribe-Romo, *J. Am. Chem. Soc.*, 2019, **141**, 11298–11303.
25 X. Y. Liu, F. Zhang, T. W. Goh, Y. Li, Y. C. Shao, L. Luo, W. Huang, Y. T. Long, L. Y. Chou and C. K. Tsung, *Angew. Chem., Int. Ed.*, 2018, **57**, 2110–2114.
26 D. Magde, G. E. Rojas and P. G. Seybold, *Photochem. Photobiol.*, 1999, **70**, 737–744.
27 A. J. Bain, P. Chandna, G. Butcher and J. Bryant, *J. Chem. Phys.*, 2000, **112**, 10435–10449.
28 D. Fairen-Jimenez, S. A. Moggach, M. T. Wharmby, P. A. Wright, S. Parsons and T. Düren, *J. Am. Chem. Soc.*, 2011, **133**, 8900–8902.
29 C. Avci, I. Imaz, A. Carne-Sanchez, J. A. Pariente, N. Tasios, J. Perez-Carvajal, M. I. Alonso, A. Blanco, M. Dijkstra, C. Lopez and D. Maspoch, *Nat. Chem.*, 2018, **10**, 78–84.
30 L. Y. Chou, P. Hu, J. Zhuang, J. V. Morabito, K. C. Ng, Y. C. Kao, S. C. Wang, F. K. Shieh, C. H. Kuo and C. K. Tsung, *Nanoscale*, 2015, **7**, 19408–19412.
31 P. Wei, L. Duan, D. Zhang, J. Qiao, L. Wang, R. Wang, G. Dong and Y. Qiu, *J. Mater. Chem.*, 2008, **18**, 806.
32 S. Wang, C. M. McGuirk, M. B. Ross, S. Wang, P. Chen, H. Xing, Y. Liu and C. A. Mirkin, *J. Am. Chem. Soc.*, 2017, **139**, 9827–9830.
33 X. Liu, N. K. Demir, Z. Wu and K. Li, *J. Am. Chem. Soc.*, 2015, **137**, 6999–7002.
34 S. Chavan, J. G. Vitillo, D. Gianolio, O. Zavorotynska, B. Civalleri, S. Jakobsen, M. H. Nilsen, L. Valenzano, C. Lamberti, K. P. Lillerud and S. Bordiga, *Phys. Chem. Chem. Phys.*, 2012, **14**, 1614–1626.
35 J. H. Cavka, S. Jakobsen, U. Olsbye, N. Guillou, C. Lamberti, S. Bordiga and K. P. Lillerud, *J. Am. Chem. Soc.*, 2008, **130**, 13850–13851.
36 X. Miao, D. Qu, D. Yang, B. Nie, Y. Zhao, H. Fan and Z. Sun, *Adv. Mater.*, 2018, **30**, 1704740.
37 F. Yuan, Z. Wang, X. Li, Y. Li, Z. Tan, L. Fan and S. Yang, *Adv. Mater.*, 2017, **29**, 1604436.
38 K. Jiang, Y. Wang, X. Gao, C. Cai and H. Lin, *Angew. Chem., Int. Ed.*, 2018, **57**, 6216–6220.
39 J. Liu, Y. Liu, N. Liu, Y. Han, X. Zhang, H. Huang, Y. Lifshitz, S.-T. Lee, J. Zhong and Z. Kang, *Science*, 2015, **347**, 970–974.